Size Polydispersity Determination in Emulsion Systems by Free Diffusion Measurements via PFG-NMR

Luigi Ambrosone,*,† Sergio Murgia,‡ Giuseppe Cinelli,† Maura Monduzzi,‡ and Andrea Ceglie†

Consorzio Sistemi a Grande Interfase (C.S.G.I.), Department of Food Technology, Università del Molise, via De Sanctis, I-86100 Campobasso (CB), Italy, Department of Chemical Science, Università di Cagliari, s.s. 554 Bivio Sestu, 09042 Monserrato (CA), Italy

Received: August 5, 2004; In Final Form: September 8, 2004

A new method to determine particle size distribution from NMR self-diffusion data is presented. The method is not subjected to the usual limitations of standard techniques, like an a priori hypothesis on the form of the distribution, or the prerequisite that suitable experimental conditions exist to enclose the whole volume fraction distribution. The new procedure, based on the measurements of free self-diffusion coefficients, was applied first by way of demonstration, to a water-in-oil emulsion system. Here, the experimental conditions were such that the data had enough information to describe the distribution function completely. Very good agreement was found for the size distribution obtained via NMR and optical microscopy data analysis. Remarkably, using the same approach in the case of a more complex oil-in-water emulsion system, for which experiments did not cover the whole range of size distribution, very good agreement was also obtained.

1. Introduction

Emulsions are colloidal systems consisting of a thermodynamically unstable dispersion, in the form of droplets, of a liquid in an immiscible continuous liquid medium. Rearrangement of the droplets that evolve toward two individual bulk liquids will occur through a net reduction in interfacial area, and such systems will separate after a period of time. Emulsifiers lower the interfacial tension between the two immiscible liquids and reduce the free-energy penalty for the liquid dispersion. This allows the achievement of metastable states that are, for all practical purposes, completely stable. The time-evolution study of such kinetically stable systems is of great technical importance. Indeed, many food, cosmetic, and pharmaceutical formulations are made up of emulsions and require the emulsion droplets to be stable over the product shelf life, which may be a year or more.

Once formed, the emulsion will phase separate as a result of several dominant breakdown processes. These are variously termed creaming (or sedimentation), flocculation (and/or aggregation), and coalescence. Since the latter affects the emulsion structure directly (droplets do not retain their individual integrity), change in droplet size with time is a fundamental measure of the extent of coalescence. Moreover, droplet size and polydispersity significantly influence the rheology of concentrated emulsions. In addition, some of the most significant properties in emulsion-based food products (appearance, texture, and flavor) are related to the size of the droplets they contain.[1] Therefore, a knowledge of the polydispersity index, that is, the particle size distribution function $P(R)$ (the fraction of particles with radius between R and $R + dR$) is crucial for a complete characterization of emulsion systems.[2,3]

Among the different techniques (e.g., electron microscopy, light scattering methods) available to measure the function $P(R)$, only nuclear magnetic resonance (NMR) so far allows distinction to be made between aggregates and large single particles. Moreover, the NMR technique is not invasive or destructive to the sample. Packer and Rees[4,5] first used NMR to provide a measure of the droplet size distribution of an emulsion in a noninvasive manner. They assumed a log-normal form for the distribution function and used a nonlinear least-squares procedure to evaluate the mean and the variance.

In the past decade, a growing effort has been made to improve the performance of NMR-based methods, occasionally coupling different sequences of radio frequency and magnetic field gradient pulses. A number of papers aimed to improve the fitting of the data sets, mostly to avoid the constraint imposed by an a priori assumption of the distribution function, has appeared.[6−10]

It has been shown recently that, under suitable conditions, the distribution function may be extracted directly from the experimental results.[7] This method, known as the *direct method*, is based on the following ansatz: if the range of the droplet size experimentally accessible (*R-interval*), determined by the experimental setup, is sufficiently large to contain the volume fraction distribution, then the experimental data will contain enough information to describe the distribution function. When it is not possible to achieve such conditions, the *direct method* model cannot be used to gain information about the distribution form.

To overcome this limitation, an innovative method based on the measurement of the free self-diffusion coefficient (D) is developed here. The method was first tested on the recently investigated water-in-oil (w/o) emulsion system, Water/Isooctane/Epikuron 200 ($W/iC_8/E_{200}$),[11,12] and then subjected to further illustrative tests by application to an oil-in-water (o/w) emulsion prepared with a delactosated acid whey powder (DAWP) obtained from dairy industry liquid waste.

2. Materials and Methods

2.1. Materials. Epikuron 200, a purified, waxlike phosphatidylcholine of soybean origin (min 92% phosphatidylcholine)

* To whom correspondence should be addressed. Telephone: +39 0874 404715. E-mail: ambroson@unimol.it.
† Department of Food Technology, Università del Molise.
‡ Department of Chemical Science, Università di Cagliari.

10.1021/jp046480o CCC: $27.50
Published on Web 11/10/2004

produced by column chromatography, was kindly supplied by Degussa BioActives and used without any further purification. Isooctane (2,2,4-trimethylpentane, 99.5% purity grade) was obtained from Carlo Erba Reagents. Sodium chloride (99.5% purity grade) and glycerol trioleate (GTO), with technical purity of 65 wt % (this reagent also contains monoglycerides and 1,3- and 1,2-diglycerides; the fatty acid chain composition is 90 wt % as oleic acid and 10 wt % as linoleic acid), were purchased from Sigma. Distilled water, passed through a Milli-Q water purification system (Millipore), was used. All the chemicals were used as received.

2.2. W/iC$_8$/E$_{200}$ Emulsion Preparation. Using an automatic blender, an opalescent yellow mixture was obtained by dissolving E$_{200}$ in *i*C$_8$ (E$_{200}$/*i*C$_8$ = 40/60 wt/wt). After a few minutes of storage in an oven at 37 °C, the mixture turned into an isotropic solution. Afterward, 30 wt % of NaCl 30 mM water solution was added to get a sample of final composition W/*i*C$_8$/E$_{200}$ = 30/42/28[13] that was emulsified through a vortex mixer (10 min at the max speed). The milky and opaque emulsion obtained was stored overnight in a thermostatic oven at 25 °C prior to NMR analysis.

2.3. Delactosated Acid Whey Powder Production (DAWP). Acid whey derived from ricotta manufacture was received from a dairy (F. Podda S.p.A., Sestu, Cagliari, Italy). In a first step of purification, the whey was centrifuged at 4 °C for 1 h at 12 000 rpm to remove the suspended material. The supernatant was then filtered, using a Gooch crucible with porosity grade of 2, and a glass filtering flask connected to a hydroaspirator vacuum pump. An ultrafiltration followed to concentrate the whey retentate by a 10-fold volume reduction. The ultrafiltration unit consisted of a Masterflex-L/S peristaltic pump operating at 2.5 bar and a flux rate of 100 mL/min coupled to a polyethersulfone membrane (Vivascience Vivaflow 200) with a molecular weight cutoff of 10 kDa. Successively, the retentate was dialyzed, using Milli-Q water and the same membrane until the lactose was completely removed. The absence of lactose was tested with the classical Fehling assay for reducing sugars. The concentrated whey was finally freeze-dried to produce a delactosated acid whey powder.

2.4. W/GTO/DAWP Emulsion Preparation. An emulsion was prepared by weighing an appropriate amount of W, GTO, and DAWP in a glass tube to obtain the desired system composition (W/GTO/DAWP, 39/58/3 wt %). This three-component system was then gently blended with a vortex mixer and, finally, mixed using an Ultra Turrax T8 equipped with an 8 mm dispersing element for 10 min at the maximum speed (25 000 rpm).

2.5. NMR Measurements. ^{1}H NMR self-diffusion measurements were performed using the pulse field gradient stimulated-echo sequence (PFGSTE technique) by means of a Bruker Avance 300 MHz (7.05 T) spectrometer at the operating frequency of 300.13 MHz, at 25 °C. A standard variable temperature control unit (with an accuracy of 0.5 °C) was used. The spectrometer is equipped with a Bruker field gradient probe DIFF30 that can reach field gradients of up to 3.0 T/m. The experiments were carried out by varying the gradient strength (g), while keeping the gradient pulse length (δ) and the gradient pulse intervals (Δ) constant. To find out the $\Phi(R)$ functions (see below), a set of PFGSTE experiments were performed using 20 different Δ values (3, 4, 5, 6, 8, 10, 20, 30, 40, 60, 80,100, 200, 300, 500, 700, 900, 1100, 1300, and 1500 ms) for the W/*i*C$_8$/E$_{200}$ emulsion, and 10 different Δ values (10, 20, 30, 50, 100, 200, 300, 500, 700, and 1000 ms) for the W/GTO/DAWP emulsion. Depending on the Δ value used, a δ between 1 and 5 ms was chosen. The echo-intensity decay of the water NMR signal in the W/*i*C$_8$/E$_{200}$ emulsion and of the NMR signals of the GTO methylene groups in the W/GTO/DAWP emulsion were measured at 16−20 different g values. It should be noted that these signals are not overlapped with any other signals in the respective ^{1}H NMR spectra.

2.6. Optical Microscopy. Optical micrographs were obtained through an optical microscope Zeiss Axioplan 2, at 25 °C. To get representative results from the system, video-enhanced microscopy was used. Such a technique combines the magnification power of the microscope with the digital image acquisition capability of a video camera. A series of images (7 pictures, 670 particles) were examined to extract the size polydispersity that was estimated by counting the droplet "average number" at the different radii in micrographs of a Thoma grating. Image-analysis software (Sigma Scan Pro, SPSS Science Software products), which provides a wide range of analytical features in addition to image enhancement, was used for digitizing the images.

3. Theoretical Background

3.1. NMR Measurements of the Self-Diffusion Coefficient. The pulsed field gradient (PFG) NMR technique, as developed by Stejskal and Tanner,[14] has been widely applied for the detection of diffusion that occurs during the time interval Δ between two gradient pulses. In this method, the NMR signal attenuation (or echo decay) is defined as the ratio of signal intensities with and without the presence of a magnetic field gradient. It is assumed that the measurement is insensitive to the diffusional process in the absence of a field gradient. Therefore, the self-diffusion coefficient can be evaluated by the following relationship:

$$E(\delta,\Delta,g,\tau_1) = e^{-2(\tau_1/T_2)}\, e^{-(\gamma g\delta)^2 D[\Delta-(\delta/3)]} \qquad (1)$$

where $E(\delta,\Delta,g)$ represents the echo attenuation, τ_1 is the RF pulse interval, δ is the duration of the applied field gradient, g is the strength of the applied gradient, and T_2 is the transverse relaxation time.

The measurement of self diffusion by the spin−echo method (PFGSE) is limited by the loss of phase coherence due to transverse relaxation. This problem may be overcome by using the stimulated-echo technique (PFGSTE), in which the experiment relies on the relatively longer longitudinal relaxation, thus providing a more extended range of time for self-diffusion measurements.[15−17] In such a situation, eq 1 becomes

$$E(\delta,\Delta,g,\tau_2,T) = e^{-2(\tau_2/T_2)-(T/T_1)}\, e^{-(\gamma g\delta)^2 D[\Delta-(\delta/3)]} \qquad (2)$$

where τ_2 and T are the constant times between the first and the second, and the second and the third 90° pulse, respectively. T_1 is the longitudinal relaxation time.

3.2. Restricted Diffusion. In a heterogeneous system, the translational diffusion of molecules is strongly influenced by the internal structure of the sample. In a confined geometry, the largest extent of diffusional displacement is limited by the size of the confinement. In principle, the goal of the experiment is quite simple: it is to measure the mean displacement of the spin-bearing molecules during the time Δ (the time scale of the experiment). In this lapse of time, the diffusion length is $L = (2D\Delta)^{0.5}$. If we assume that there is a single length R in the confined geometry, deviations from free diffusion are seen for $L \geq R$. This fact can be used to obtain information about the length scale from the echo attenuation through equation:

$$E(\delta,\Delta,g,R) = \exp\left[\frac{-2(\gamma g)^2}{D}\sum_{m=1}^{\infty}\frac{1}{\xi_m^4(\lambda_m^2-2)}f_m(\delta,\Delta,R)\right] \quad (3)$$

where

$$f_m(\delta,\Delta,R) = 2\delta - \frac{2 + e^{-\xi_m^2 D(\Delta-\delta)} - 2\,e^{-\xi_m^2 D\Delta} - 2\,e^{-\xi_m^2 D\delta} + e^{-\xi_m^2 D(\Delta+\delta)}}{\xi_m^2 D} \quad (4)$$

are functions which depend on the experimental parameters δ and Δ, and on the droplet radius R.[7] The entities $\lambda_m = \xi_m R$ are the mth roots of the equation $J_{3/2}(\lambda) - \lambda J_{5/2}(\lambda) = 0$ with $J_p(x)$ being the Bessel function of order p.

It should be noted that L, the mean displacement of the spin-bearing molecules during a fixed-time interval (Δ), must not be understood as a physical barrier for the spins, but as a numerical-experimental limitation. In other words, it is a device to gain information on a region of droplet distribution that is not accessible experimentally.

It is also worth stressing that eq 3 is obtained under the constraint of the *reflecting barrier*,[7] thus, the surface relaxivity of the droplets is zero. This implies that T_1 and T_2 relaxation times are independent of droplet size. Hence, these relaxation terms in eqs 1 and 2 can be included in the normalization constant provided that, in the experimental run, τ_1 or τ_2 and T are kept constant. Therefore, under these conditions, eqs 1 and 2 are fully equivalent to evaluate the self-diffusion coefficient.

In polydisperse systems, the droplets of each size will obey eq 3. Thus, the measured echo attenuation (I) is a sum of the echo contributions from the various droplets weighed through the volume fraction of each droplet size:

$$I = \int_0^{\infty} E(\delta,\Delta,g,R)\Phi(R)\,dR \quad (5)$$

where $\Phi(R)$ is the volume fraction distribution function for which

$$\int_0^{\infty} \Phi(R)\,dR = 1 \quad (6)$$

As pointed out in ref 7 and references therein, to obtain an acceptable result from the NMR experiment, it is necessary to choose the experimental conditions to have an R-interval sufficiently large compared to the distribution width (see Introduction).

Generally, ∞ in eq 5 is replaced with L since this value fixes such an R-interval experimentally. In other words, it is assumed that all the spins in the sample experience restricted diffusion. When the particle size distribution function $P(R)$ is sufficiently broad, these conditions can no longer be achieved. Consequently, the procedure to obtain the volume fraction distribution function from NMR results has to be modified.

3.3. Computational Procedure. For very broad $P(R)$, NMR experiments do not contain enough information to allow the inversion of eq 5. The emulsion structure and the type of spectrometer limit the maximum L that can be experimentally attained. The crucial point is that the echo attenuation is related to $\Phi(R)$ and not to $P(R)$. As a consequence, a broad $\Phi(R)$ might not be sufficiently defined within the experimental limits although, in the same situation, $P(R)$ is still itself well described (see Figure 1).

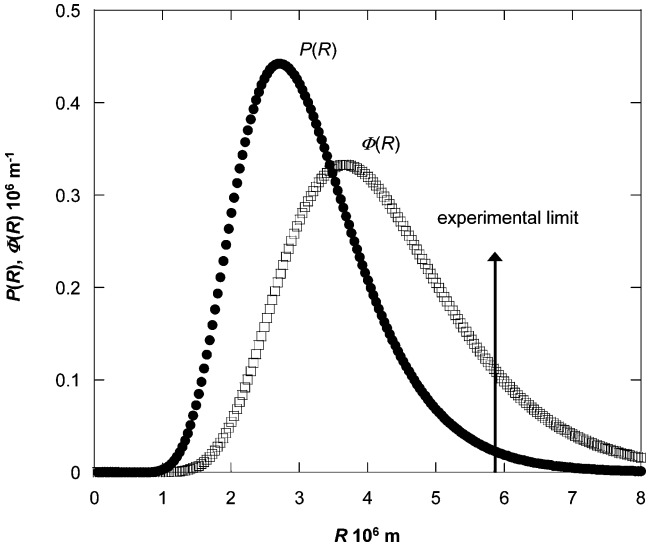

Figure 1. Influence of the NMR experimental conditions on the accuracy of particle $P(R)$ and volume $\Phi(R)$ distribution functions ($P(R)$ and $\Phi(R)$ are simulated functions). If the experimental conditions do not span and enclose the entire $\Phi(R)$ function, the size distribution determination will be affected by a large error, that is, the R-interval is underestimated.

It follows that, when $\Phi(R)$ is broad so that it is not completely contained within the experimental limits, the *direct method* cannot be used to solve eq 5. To study this case the method has been extended and generalized here.

First the integral of eq 5 was split into two parts:

$$I = \int_0^L E(\delta,\Delta,g,R,)\Phi(R)\,dR + \int_L^{\infty} E(\delta,\Delta,g,R)\Phi(R)\,dR \quad (7)$$

The first integral is the contribution to the echo attenuation coming from spheres with radii $R \le L$. It, therefore, includes the restricted part of the diffusional motion. The second is the contribution of spheres with $R > L$, that is to say, the free diffusion. Thus, eq 7 can be rewritten as

$$I = \int_0^L E_{\text{rest}}(\delta,\Delta,g,R)\Phi(R)\,dR + \int_L^{\infty} E_{\text{free}}(\delta,\Delta,g)\Phi(R)\,dR \quad (8)$$

where $E_{\text{rest}}(\delta,\Delta,g,R)$ is the term due to restricted diffusion given by eq 3, while $E_{\text{free}}(\delta,\Delta,g)$ is the term due to free diffusion given by eq 2.

Since $E_{\text{free}}(\delta,\Delta,g)$ is independent of R, and $\Phi(R)$ is normalized (see eq 6), eq 8 can be rearranged in the following form:

$$I = \int_0^L E_{\text{rest}}(\delta,\Delta,g,R)\Phi(R)\,dR + \alpha(L)E_{\text{free}}(\delta,\Delta,g) \quad (9)$$

where

$$\alpha(L) = \int_L^{\infty} \Phi(R)\,dR \quad (10)$$

is the volume fraction of molecules that diffuse into spheres with radius $R > L$.

Equation 9 shows that the *direct method* may also be used to obtain $\Phi(R)$ through an iterative procedure. However, since this work was aimed at obtaining a rapid procedure that can be used routinely to estimate the degree of polydispersity in emulsion systems, the use of an averaged procedure was preferred.

Applying a mean theorem,[18] eq 9 can be rewritten as

$$I = (1 - \alpha(L))E_{rest}(\delta,\Delta,g,L') + \alpha(L)E_{free}(\delta,\Delta,g) \quad (11)$$

where $E_{rest}(\delta,\Delta,g,L')$ is the echo decay evaluated for $R = L'$, that is, a radius value within the interval $[0, L]$. Here, the quantity $(1 - \alpha(L))$ represents the volume fraction of spins which experiences restricted diffusion.

As shown in ref 7 (eq 8), for $D\delta < L^2$ the following relationship can be introduced

$$\sum_{m=1}^{\infty} \frac{1}{\xi_m^4(\lambda_m^2 - 2)} f_m(\delta,\Delta,R) \approx \Gamma\delta^2 \quad (12)$$

with

$$\Gamma \approx \frac{\mu_2 D}{10} \quad (13)$$

where μ_2 is the second moment of the distribution $\Phi(R)$. Therefore, the restricted term in eq 11 can be written as

$$E_{rest}(\delta,\Delta,g,L') = e^{-(\gamma g\delta)^2\Gamma} \quad (14)$$

Finally, taking into account eqs 2 and 14, eq 11 becomes:

$$I = (1 - \alpha(L))\, e^{-\Gamma'(\gamma g\delta)^2[\Delta-(\delta/3)]} + \alpha(L)\, e^{-(\gamma g\delta)^2 D[\Delta-(\delta/3)]} \quad (15)$$

where

$$\Gamma' = \frac{\Gamma}{\Delta - (\delta/3)}$$

is a parameter depending only on Δ and δ, which are kept constant during a typical experiment.

4. Results and Discussion

4.1. w/o Emulsion: The Test Case. The w/o emulsion sample W/iC$_8$/E$_{200}$ was prepared as described in the Materials and Methods section. As already reported,[11,12] this system, as viewed through the microscope, looked like a coarse dispersion of droplets in a continuous medium (see Figure 2). The observation through a polarizing lens revealed the presence of Maltese crosslike structures, a texture typically associated with vesicular/lamellar structures. It is worth noticing that the use of a NaCl (30 mM)−water solution instead of pure water caused an increase of the droplet diameter, thus allowing an easier analysis. No relevant effect on pure water self-diffusion coefficient because of the salt addition was detected. The NMR self-diffusion data for the water species in the emulsion sample W/iC$_8$/E$_{200}$ are shown in Figure 3. The measured echo attenuation I/I_0 vs the acquisition parameters are reported for different Δ values. The echo attenuation of the water signal strongly depends on the diffusion observation time Δ. These findings confirm that water molecules experience restricted diffusion inside droplets.

The problem of the numerical determination of the distribution function $\Phi(R)$ is the evaluation of the coefficient α in eq 9. With this in mind, the experimental echo decays were fitted by a biexponential function for each different Δ value. In all the cases the mean error was within 1%.

Then, the fraction of spins $(1 - \alpha)$ experiencing restricted diffusion was obtained by eq 15 for the different $L = (2D\Delta)^{0.5}$ values ($D = 2.3 \times 10^{-9}$ m^2 s^{-1} is the pure water self-diffusion coefficient). Data reported in Figure 4a correspond to the droplet fraction with $R \leq L$ and, therefore, represent the entire probability (cumulative sum) of particles with $\Phi(R \leq L)$.

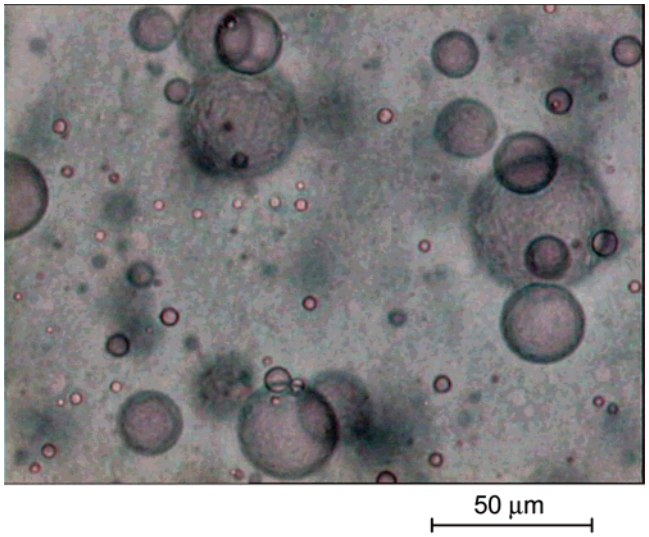

Figure 2. W/iC$_8$/E$_{200}$ emulsion. Light microscopy photograph at 25 °C.

Since the probability density must be obtained, eq 10 was derived, thus obtaining

$$\Phi(R) = \frac{d(1 - \alpha)}{dL} \qquad \text{for } R \leq L \quad (16)$$

Experimental data are always affected by errors. These errors prevent a simple differential technique from being used to obtain the derivative of eq 16. To get a good estimate of the derivative at a point, a function must be fitted to several data points on both sides of that point. Then, the resulting function can be differentiated analytically. To do this, it is convenient to start at the top of the table of data and move stepwise down, evaluating the derivative at each center point by "arc moving" or "strip moving".[19]

Furthermore, all experimental data require smoothing before differentiation is performed. Smoothing is performed here by passing a least-squares polynomial through the data points to determine the polynomial coefficients and then replacing the experimental points with those calculated from the polynomial. The data points were smoothed, using five points in the movable strip and a third-degree polynomial.[20] The smoothing was terminated at the stage where the random error was minimized. Application of this procedure to data in Figure 4a gives the graph reported in Figure 4b.

Figure 5 shows the distribution $\Phi(R)$ obtained deriving data from Figure 4b according to eq 16. This diagram will be the more accurate the more the curve of Figure 4b approaches the asymptotic value 1 (i.e., all the spins in the sample experience restricted diffusion). This condition corresponds to a good choice of the R-interval in the *direct method*.[7] However, the last part of the curve is flat and can be extrapolated with a relatively small error.

The validity of the method was tested, comparing NMR diffusion data with those acquired from optical microscopy analysis. Results from optical microscopy overlap very well with those obtained from NMR in Figure 5. The good agreement between the two series of results shows that the approach developed here can be used to obtain both the distributions $\Phi(R)$ and $P(R)$ in systems where all the Φ values can be experimentally explored.

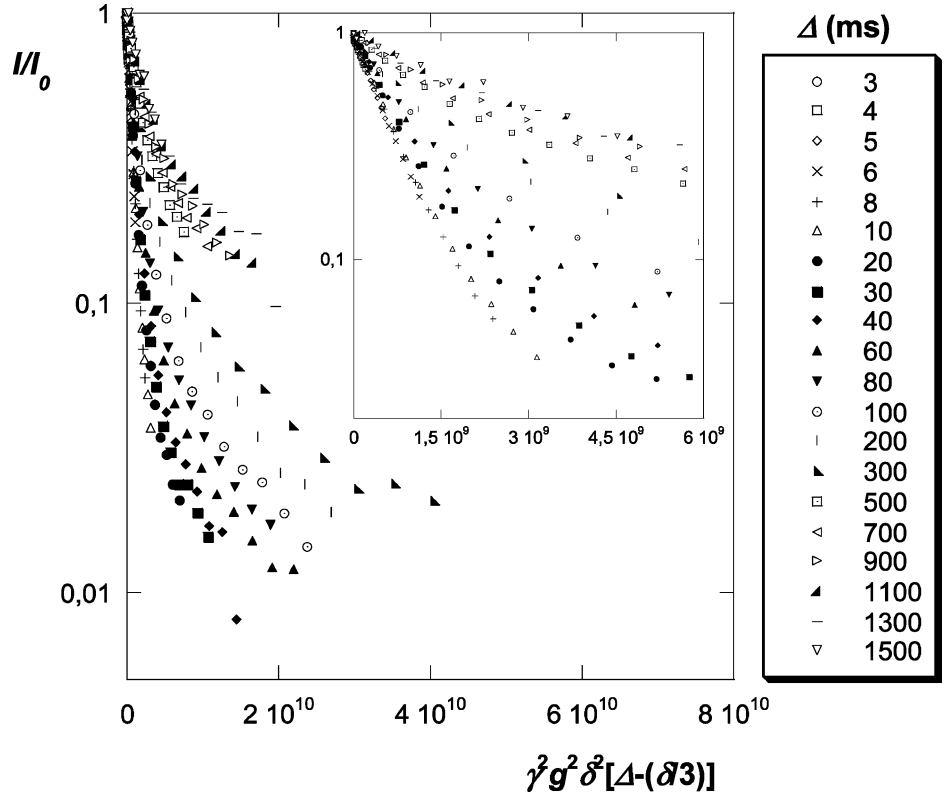

Figure 3. W/iC_8/E_{200} emulsion. Normalized signal attenuations with increasing gradient strength in the PGSTE NMR experiments at different Δ values (Δ = 3, 4, 5, 6, 8, 10, 20, 30, 40, 60, 80, 100, 200, 300, 500, 700, 900, 1100, 1300, and 1500 ms). (Inset) Enlargement of the region at low *g* values.

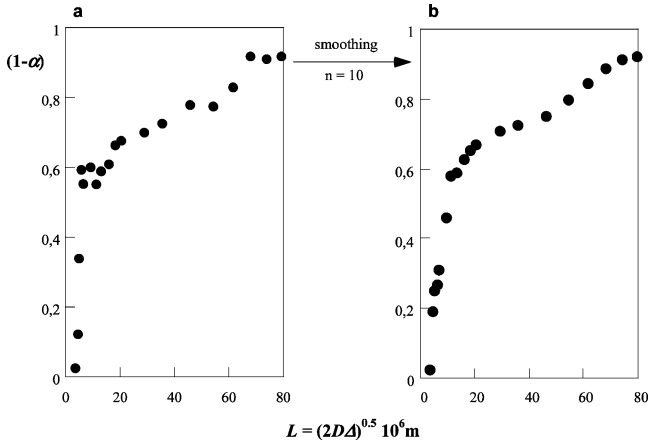

Figure 4. W/iC_8/E_{200} emulsion. (1 − α) vs $L = (2D\Delta)^{0.5}$, where *D* is the water self-diffusion coefficient. (a) Cumulative sum obtained from NMR data. (b) Effect of smoothing on experimental data; *n* is the number of times that smoothing is applied.

4.2. o/w Emulsion: A Case where the Whole Φ(*R*) Cannot Be Determined. With this established, the same approach was then used to evaluate the distribution Φ(*R*) of an o/w emulsion prepared with a protein-rich concentrate obtained from dairy industry waste (see Materials and Methods section). This more complicated system poses a challenging test.

Generally, information about the free self-diffusion coefficient of the dispersed phase is obtained either by assuming an ideal behavior of the liquid inside the droplets or directly by measuring the diffusion coefficient after macroscopic demixing. However, it is often difficult to obtain the chemical composition of the dispersed phase of a complex multicomponent emulsion. Consequently, it is important to be able to compute *D* directly from experimental data.

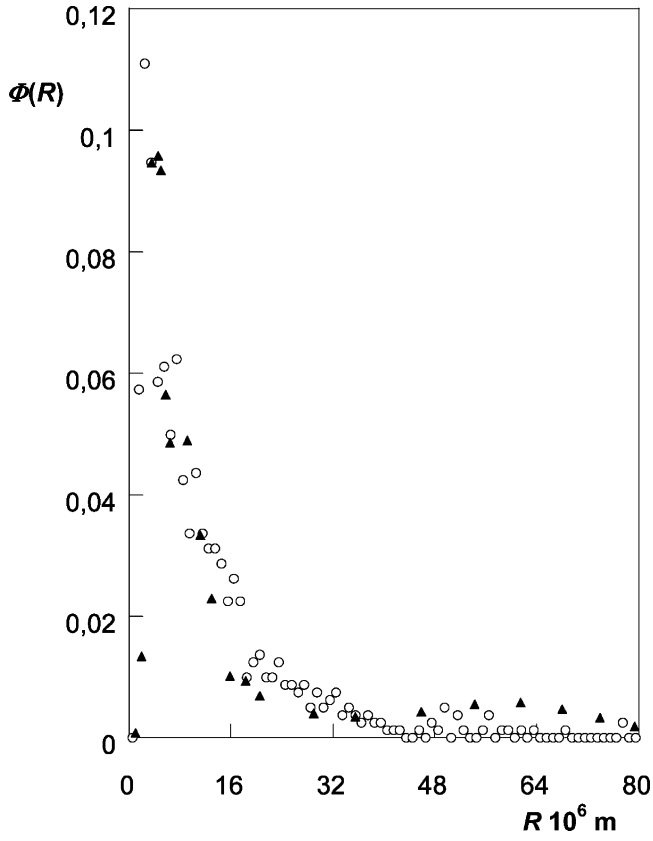

Figure 5. W/iC_8/E_{200} emulsion. Comparison of the volume fraction distribution Φ(*R*) obtained through NMR (▲) and optical microscopy (○) data analysis.

It is evident from eq 15 that, if the experimental data are fitted by two exponentials having three adjustable parameters

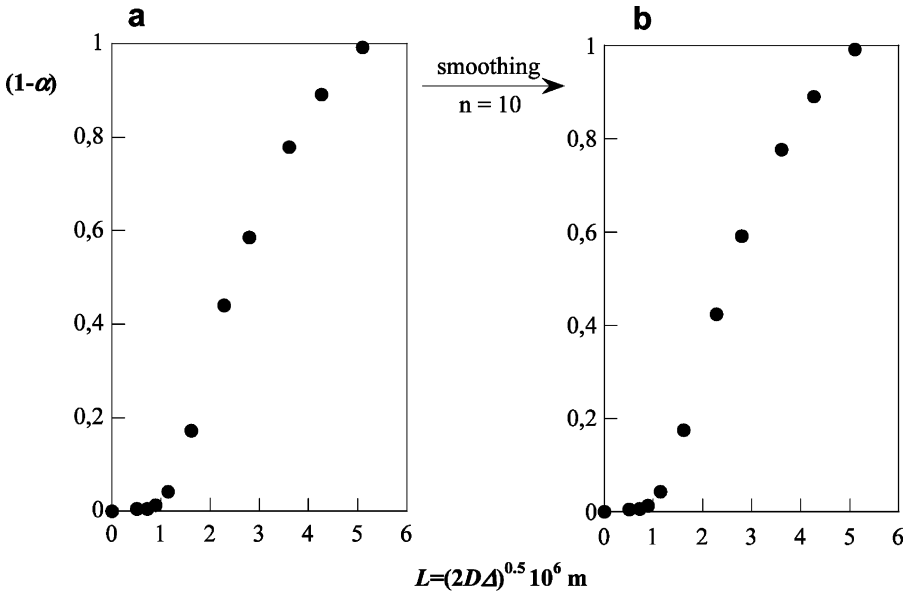

Figure 6. W/GTO/DAWP emulsion. $(1 - \alpha)$ vs $L = (2D\Delta)^{0.5}$, where D is the oil species self-diffusion coefficient. (a) Cumulative sum obtained from NMR data. (b) Effect of smoothing on experimental data; n is the number of times that smoothing is applied.

(D, α, Γ'), D can be calculated by means of a least-squares procedure. However, the numerical fluctuations make it difficult to apply this method in evaluating D and α simultaneously by a biexponential fitting. Therefore, all experimental results were fitted using two exponentials with four adjustable parameters (two independent preexponential parameters with no physical meaning and two exponential parameters). A first step allowed D to be obtained from the exponential parameter that was showing the lowest fluctuations. The average of the fluctuating values was chosen as the best D value. During a second step, the D value was kept constant, and the experimental data were refitted by only two adjustable parameters (α, Γ') to evaluate α. The procedure applied to W/GTO/DAWP emulsion led to an average $D = (1.3 \pm 0.2) \times 10^{-11}$ m^2 s^{-1} for the oil species self-diffusion coefficient. It should be remarked that this finding is very close to the value $D = (1.00 \pm 0.05) \times 10^{-11}$ m^2 s^{-1} obtained for pure GTO at 25 °C through a PGSTE NMR experiment.

Parts a and b of Figure 6 show, respectively, the cumulative sum before and after smoothing for the W/GTO/DAWP emulsion. From these figures it is clear that, in this case, because of experimental limitations the curve does not reach a plateau, that is, the whole range of the $\Phi(R)$ values cannot be enclosed.

The volume fraction distribution function $\Phi(R)$, obtained by differentiating data of Figure 6b, is shown in Figure 7 in comparison with the corresponding result from optical microscopy analysis. Despite the low number of data points, a good agreement between the two techniques is again observed. This result is quite remarkable and provides a further assessment of the validity of the proposed approach. Indeed, a reliable estimate of the polydispersity index was obtained for an emulsion system for which the experimental setup did not allow full access to the entire range of $\Phi(R)$ values.

4.3. Form of the Size Distribution. As to the form of the distribution function, it is worth considering that, since for a log-normal distribution the moments are given by $\mu_n = R_0^n e^{0.5n^2\sigma^2}$, with $n = 1, 2, \ldots$, a plot of $\ln(\mu_n^{1/n})$ versus n can be used to verify that the emulsion system falls within such a distribution class.

In the case of W/iC_8/E_{200} emulsion, data reported in Figure 8a cannot be described by a straight line, thus ruling out the choice of a log-normal distribution. Obviously, other forms of the distribution function $\Phi(R)$ should be suggested, but this is beyond the aims of the present work. Conversely, the result for W/GTO/DAWP emulsion reported in Figure 8b shows a good linear fit, thus indicating that the log-normal distribution describes the system accurately as found for many food emulsions.[21]

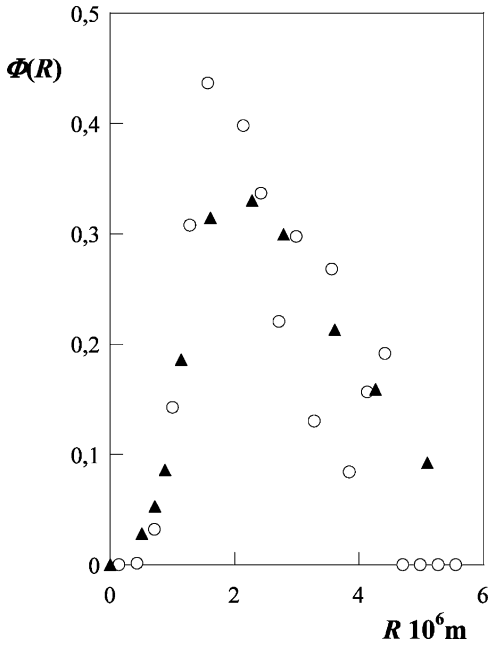

Figure 7. W/GTO/DAWP emulsion. Comparison of the volume fraction distribution $\Phi(R)$ obtained through NMR (▲) and optical microscopy (○) data analysis.

5. Comparison with Alternative Methods and Concluding Remarks

In this context, it should be mentioned that other promising methods have recently been proposed. The use of a combination of CPMG-PGSE low-field NMR experiments, accompanied by sophisticated data analysis,[10] and regularization methods using fast diffusion measurements (Difftrain sequence)[8,9] are some

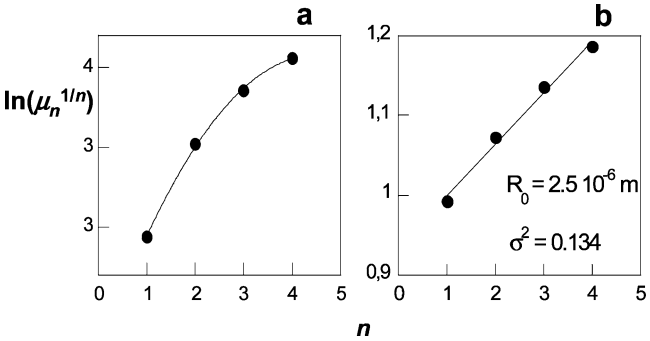

Figure 8. Assessment of the log-normal distribution for (a) W/iC_8/E_{200} and (b) W/GTO/DAWP systems. R_0 and σ indicate, respectively, the geometric mean and the geometric standard deviation from $\Phi(R)$ in Figure 7. R and $\Phi(R)$ are expressed in μm and μm^{-1}, respectively.

interesting examples. For instance, in the case of the CPMG-PGSE combined method,[10] size distributions from microphotography were generally in good agreement with those from NMR data analysis using either a modified form of the bimodal Weibull cumulative probability distribution function or a log-normal distribution. This approach is certainly useful, particularly with low-resolution magnets (around 0.05 T). In addition, the method overcomes the problem arising from the high intensity of the NMR signals from the continuous phase and, more importantly, allows for a larger range of droplet size (0.01−300 μm) than usual PGSE experiments allow. However, to the best of our knowledge, only the regularization methods recently reported[8] and used to evaluate emulsion droplet size distribution from Difftrain sequence experiments[9] seem to overcome the problems related to an "a priori" choice of the distribution function form.

Compared with all these perhaps equally valid approaches, the method developed here contains some new elements and advantages which deserve note:

1. The form of the distribution function is not assumed as in the case of regularization methods. Nonetheless, the droplet size distribution can be obtained satisfactorily when compared with another NMR-independent method. It is also done without invoking any assumed mathematical form.

2. The present method also gives satisfactory results in cases where the experimental data do not cover the whole range of droplet size because of experimental limitations.

Finally, it should be mentioned that the approach used in this paper is limited to diluted emulsions[7] where the volume fraction of droplets does not exceed 74%. For concentrated emulsions, the molecules may jump from one droplet to another, that is, the barriers are permeable and the surface relaxivity is finite. In these cases, the molecules at interfaces may have considerably different relaxation times compared to those in bulk liquids. In addition, it should be considered that a close packing of small spheres is characterized by a high surface area-to-volume ratio. Consequently, T_1 and T_2 become dependent on cavity radius and cannot be considered constant.

Acknowledgment. C.S.G.I., M.I.U.R. legge 488, and P.R.I.N. 2003 are acknowledged for financial support. B. W. Ninham is thanked for useful comments on the manuscript.

References and Notes

(1) McClements, D. J. *Food Emulsions: Principles, Practice and Techniques*; CRC Press: Boca Raton, 1999.

(2) Söderman, O.; Lönqvist, I.; Balinov, B. NMR Self-Diffusion Studies of Emulsion Systems. Droplet Sizes and Microstructure of the Continuous Phase. In *Emulsions - A Fundamental and Practical Approach*; Sjoblom, J., Ed.; Kluwer Academic Publishers: Dordrecht, 1992; p 239.

(3) Balinov, B.; Urdahl, O.; Söderman, O.; Sjöblom, J. *Colloids Surf., A* **1994**, *82*, 173.

(4) Packer, K. J.; Rees, C. *J. Colloid Interface Sci.* **1972**, *40*, 206.

(5) Callaghan, P. T.; Jolley, K. H.; Humphrey, R. S. *J. Colloid Interface Sci.* **1983**, *93*.

(6) Fourel, I.; Guillement, J. P.; Botlan, D. L. *J. Colloid Interface Sci.* **1995**, *169*, 119.

(7) Ambrosone, L.; Ceglie, A.; Colafemmina, G.; Palazzo, G. *J. Phys. Chem. B* **2000**, *104*, 786 and references therein.

(8) Hollingsworth, K. G.; Johns, M. L. *J. Colloid Interface Sci.* **2003**, *258*, 383.

(9) Buckley, C.; Hollingsworth, K. G.; Sederman, A. J.; Holland, D. J.; Johns, M. L.; Gladden, L. F. *J. Magn. Reson.* **2003**, *161*, 112.

(10) Peña, A. A.; Hirasaki, G. J. *Adv. Colloid Interface Sci.* **2003**, *105*, 103.

(11) Angelico, R.; Ceglie, A.; Colafemmina, G.; Delfine, F.; Olsson, U.; Palazzo, G. *Langmuir* **2004**, *20*, 619.

(12) Stefan, A.; Palazzo, G.; Ceglie, A.; Panzavolta, E.; Hochkoeppler, A. *Biotechnol. Bioeng.* **2003**, *81*, 323.

(13) Angelico, R.; Ceglie, A.; Hochkoeppler, A.; Palazzo, G.; Stefan, A. Macroemulsioni acqua in olio a lunga stabilità, loro preparazioni ed uso (Long-term stability in water macroemulsions, their preparation and use).Italian Patent FI 2001A16, 2001.

(14) Stejskal, E. O.; Tanner, J. E. *J. Chem. Phys.* **1965**, *42*, 288.

(15) Callaghan, P. T. *Principles of Nuclear Magnetic Resonance Microscopy*; Clarendon Press: Oxford, 1991.

(16) Stilbs, P. *Prog. Nucl. Magn. Reson. Spectrosc.* **1987**, *19*, 1.

(17) Dvinskikh, S. V.; Furó, I.; Sandström, D.; Maliniak, A.; Zimmermann, H. *J. Magn. Reson.* **2001**, *153*, 83.

(18) Smirnov, V. I. *Kurs vyšej matematiki Vol. I*, Italian translation ed.; Editori Riuniti: Roma, 1977.

(19) Bachvalov, N. S. Čislennye metody, Italian Translation ed.; Editori Riuniti: Roma, 1981.

(20) Hershey, H. C.; Zakin, H. L.; Simha, R. *Ind. Eng. Fundam.* **1967**, *6*, 413.

(21) Orr, C. In *Encyclopedia of Emulsion Technology*; Becker, P., Ed.; Dekker: New York, 1988; Vol. 3; p 137.